BIOCHEMISTRY
including biophysical chemistry & molecular biology

Article

pubs.acs.org/biochemistry

A Cyclic Mimic of HIV Tat Differentiates Similar TAR RNAs on the Basis of Distinct Dynamic Behaviors

Jia Lu,[†] Larry Nguyen,[‡] Liang Zhao,[†] Tianbing Xia,[†] and Xin Qi*[,‡]

[†]Department of Molecular and Cell Biology, The University of Texas at Dallas, Richardson, Texas 75080, United States
[‡]Department of Medicinal Chemistry, College of Pharmacy, University of Florida, Gainesville, Florida 32610, United States

ABSTRACT: Efforts toward the development of RNA-based drug leads have been challenging because of the complexity and dynamic nature of RNA structures as therapeutic targets. The transactivation response (TAR) RNA and cognate Tat protein of HIV have long been recognized as promising antiviral targets, and recent works have identified potentially potent inhibitors of the viral RNA−protein interaction. A new class of such inhibitors, conformationally constrained cyclic peptide mimetics of Tat, has been demonstrated to inhibit the HIV life cycle. We have previously probed the complexity and dynamics of TAR RNAs in their free states, as well as conformational shifting by various peptide and small molecule ligands. In this work, we have used an ultrafast dynamics approach to probe the interactions between TAR RNAs and one of the representatives of cyclic peptide inhibitors, L22. Our studies demonstrated that cyclic L22 specifically recognizes TAR RNAs with a unique single binding site compared to two binding sites for linear Tat protein. Although both Tat and L22 bind to the TAR RNAs as a β-hairpin structure, cyclization in L22 allows it to be a more efficient ligand from a population shifting perspective. This study provided unique insights into drug design with desired properties to differentiate similar structures based on distinct dynamic behaviors.

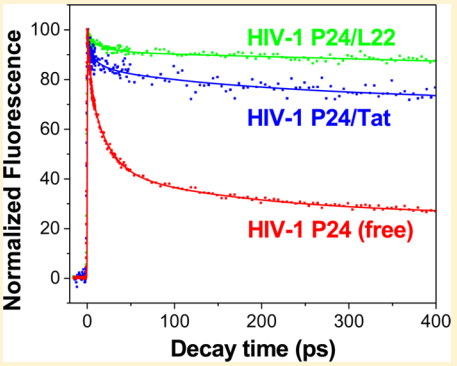

The interaction of HIV TAR RNA and Tat protein has been one of the most classical paradigms and a rich source of information for studying the role of RNA conformational dynamics, conformational changes, and their impacts on RNA functions.[1−7] The functional importance of TAR−Tat interactions for the HIV viral life cycle stimulates efforts to discover potent inhibitors to disrupt this regulatory RNA element, but efforts in this direction are still in their early stages. Various unnatural peptide mimics have been developed as the agents for targeting HIV TAR RNAs and have potential as new classes of antiviral therapeutic compounds. In particular, a Tat-derived arginine-rich oligomeric peptide/peptoid hybrid,[8,9] peptoid amide and ester analogues,[10] D-peptide,[11,12] β-peptide,[13] and cyclic peptides[14−21] have been explored intensively. These compounds have nanomolar to micromolar affinities for HIV or BIV TAR RNAs, comparable to that of the TAR RNA binding domain of the Tat proteins, and are shown to block formation of the cognate TAR−Tat complex *in vitro*[8,11,15,19,21] and inhibit Tat-dependent transactivation or HIV replication in cellular assays.[8,9,12,21] Available evidence has shown that these compounds bind at the Tat binding site of TAR RNAs[8,11,12,14,19] and induce conformational changes in the bulge region.[8,19]

The first efforts of designing conformationally constrained cyclic peptides were to target BIV TAR RNA.[14,15,17,19] These cyclic peptides selected against BIV TAR RNA had various specificities toward BIV and HIV TAR RNAs. In the complexes,[16] the structure of the RNA component is very similar to that of the complex with the natural Tat peptide. The bound β-hairpin structures of the cyclic peptides[14−17] are similar to that of the linear Tat peptide in that they bind as a β-hairpin.[22] A critical contact between the bulged U10 of the base triple and an Ile residue of Tat (Ile79) is maintained by an equivalent Ile residue (Ile10) of the BIV2 cyclic peptide, where the burial of its side chain is the main driving force for the RNA conformational transition. Unexpectedly, however, the bound cyclic peptide adopts the opposite orientation compared to that of the linear peptide,[16] suggesting that an alternative strategy can be used in the design of high-affinity compounds that may have therapeutic values.

The molecular recognition principles learned in the efforts to target BIV TAR RNA were quickly expanded to target HIV-1 TAR RNA.[17] One of the representative high-affinity (nanomolar) inhibitors, L22 (Figure 1), has been shown by NMR studies that it forms a very stable β-hairpin and retains this structure in complex with HIV-1 TAR. The L22 binds to the major groove of TAR and as its precursor, in the opposite orientation of Tat in the complex.[19] The base triple between U23 and the A27/U38 base pair is conserved, and analogous to that of the BIV2 peptide[16] where Ile10 buries its methyl groups against the base triple. Peptide binding extrudes C24 and U25, allowing the coaxial stacking of the two helical stems. C24 interacts with the side chain of Lys6 and is buried in a small pocket, while U25 is flipped and exposed to solution. From the point of view of RNA dynamics, L22 was shown to induce

Received: March 26, 2015
Revised: May 24, 2015
Published: May 28, 2015

DOI: 10.1021/acs.biochem.5b00325
Biochemistry 2015, 54, 3687−3693

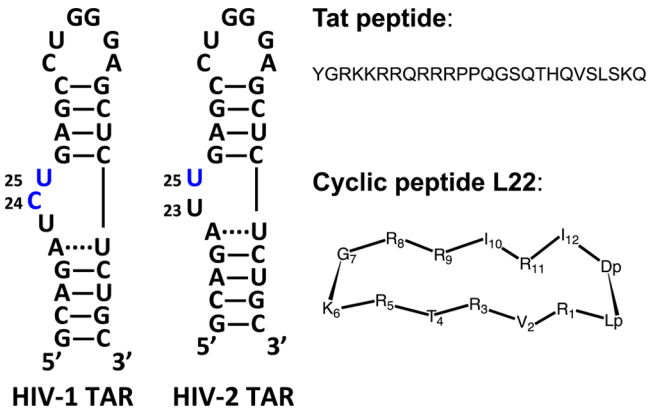

Figure 1. Sequences and secondary structures of HIV-1 and HIV-2 TAR RNA models and sequences of Tat and L22 peptides. All numberings of the RNAs are based on that of HIV-1 TAR. Bases colored blue are labeled with 2-aminopurine (2AP).

similar changes in increased dynamics of C24 and U25 within the bulge region of HIV-1 TAR RNA compared to the Tat peptide, but it induces unique decreased levels of motion in the apical loop as an additional strategy for achieving specificity,[18−20] where extending the peptide caused it to slide down the major groove of the RNA to maintain critical contacts.[20] Because of their constrained conformations in both free and RNA-bound forms, L22 and other cyclic peptides represent a new class of compounds with high potency and selectivity, as well as low toxicity. They hold great promise in the global battle of HIV treatment and warrant further biophysical characterizations of the RNA targeting mechanism.

We have recently developed ultrafast dynamics-based approaches[23,24] to dissect the dynamic behaviors of different biological systems, particularly RNA systems.[6,7,25−32] Using these approaches, we have previously conducted detailed analysis of the conformational complexity of HIV TAR and related 7SK RNAs and the changes in the conformational distribution upon binding of various ligands.[6,7] We have demonstrated that in HIV TAR RNA, the ligand-free state samples multiple families of conformations with different base stacking patterns around the functionally critical bulge region. Binding of Tat stabilizes a conformation that features the coaxial stacking, shifting equilibrium toward this state, while other states still coexist as an ensemble. The conformational transition mechanism of Tat binding manifests itself as conformational capture.[2,3,6,7,33−38] In this study, we took advantage of the TAR−L22 complex as a new model system to further our understanding of RNA dynamics and lay the foundation for drug design to target similar structures based on distinct dynamic behaviors.

EXPERIMENTAL PROCEDURES

Materials. All of the model TAR RNA constructs were purchased from Dharmacon (Lafayette, CO) and purified by PAGE. The sequences and secondary structures of the RNA constructs are shown in Figure 1. RNA concentrations were calculated from UV absorbance measurements at 260 nm using extinction coefficients provided by Dharmacon. The oligos were dissolved in sodium phosphate buffer [20 mM sodium phosphate, 25 mM NaCl, and 0.1 mM EDTA (pH 6.8)] and annealed by being heated to 95 °C and held for 1.5 min, and then snap cooled on ice. The basic region of Tat protein was obtained from the University of Texas Southwestern Medical Center Peptide Facility. The peptide was synthesized using Fmoc chemistry. The crude product was purified by high-performance liquid chromatography and lyophilized to remove failure sequences and impurities such as TFA to prevent its potential effects on peptide properties,[39] and its identity was confirmed by mass spectrometry. The concentration of the peptide was determined by absorbance at 280 nm using the tyrosine residue. Cyclic peptide L22 was initially a gracious gift from G. Varani's laboratory at the University of Washington (Seattle, WA).[17,20] Additional peptide material of L22 was obtained from The University of Texas Southwestern Medical Center Peptide Facility using the same method above.

Steady State Fluorescence Spectroscopy. Steady state fluorescence measurements were performed using a Shimadzu RF 5301 spectrofluorophotometer equipped with a temperature control module that maintains the sample temperature at 25 °C for all measurements, and the samples were constantly stirred during the collection of data. RNA solutions from 100 to 200 nM were used for titration. The excitation wavelength was 320 nm, and the emission wavelength was 370 nm. Titrations were conducted by adding 1−4 μL aliquots of Tat or L22 peptides from a 5, 20, 40, or 180 μM stock solution, and the fluorescence intensity of the buffer was subtracted from that of the samples. Between each aliquot of ligand, a 3 min period was allowed for the binding reaction to reach equilibrium. All measurements were performed in at least triplicate. The fluorescence intensity at 370 nm was plotted versus ligand concentration and analyzed using Dynafit.[40]

Femtosecond Time-Resolved Fluorescence Spectroscopy. Femtosecond pulses (120 fs, 800 nm, 2.3 mJ) are generated from a Ti:sapphire laser system (Spectra Physics). The pulse is split equally into two beams, with one beam used to pump one optical parametric amplifier (OPA), and the output signal is quadrupled to generate the excitation pump pulse at 320 nm. The remainder of the fundamental 800 nm is used as the probe pulse. The RNA concentration of all femtosecond samples was 120 μM. The emission from the sample cell is collected by a pair of parabolic focus mirrors and mixed with the probe pulse in a BBO crystal (barium borate crystal). For magic angle fluorescence measurements, the pump beam polarization was set at the magic angle (54.7°) with respect to fluorescence polarization set by the BBO crystal, to prevent complications from orientational motion. The up-converted signal at 257 nm (up-converted from 380 nm) is detected by a photomultiplier after passing through a double-grating monochromator. The fluorescence decay profiles were fit to a sum of multiple-exponential functions convoluted by the following Gaussian instrument response function:[24]

$$F(t) = \sum_{i=1}^{n} A_i \exp\left(-\frac{t - t_0}{\tau_i}\right) \times \exp\left(\frac{\Delta^2}{4\tau_i^2}\right) \left[1 + \mathrm{erf}\left(\frac{t - t_0 - \Delta^2/2\tau_i}{\Delta}\right)\right]$$

where τ_i and A_i are the decay lifetimes and pre-exponential amplitudes, respectively, for the ith decay component; t_0 is time zero; Δ is the width of the instrument response function (cross correlation, typically 500−600 fs determined by recording the Raman emission profile for solvent water); and erf is the error function. The femtosecond transients were collected up to 400 ps, and the final profiles were the averages of more than 200

DOI: 10.1021/acs.biochem.5b00325
Biochemistry 2015, 54, 3687−3693

transients. Mathematical software Scientist was used to analyze the ultrafast dynamics data.[6]

RESULTS AND DISCUSSION

L22 Binds both HIV-1 and HIV-2 TAR RNAs at a Unique Single Binding Site. Using the HIV TAR RNA model constructs (Figure 1), we have previously shown by ITC and steady state fluorescence titrations[6,7] that the natural linear Tat peptide from HIV-1 binds both HIV-1 and HIV-2 TAR RNAs with high affinities, while it can form 1:1 and 1:2 complexes indicating two sets of binding sites. The first is a specific binding site with low nanomolar binding affinity, and the second is a nonspecific binding site with micromolar binding affinity.

Figure 2 shows the comparison of the steady state fluorescence titration profiles between the Tat peptide and the cyclic mimic L22 binding to both HIV-1 and HIV-2 TAR RNAs with fluorescent probe 2-aminopurine (2AP) incorporated at the bulge bases (HIV-1 P24, HIV-1 P25, and HIV-2 P25). L22 binds to these two RNAs with similar dissociation constants (44−63 nM) with little discrimination (Table 1). In contrast to the linear Tat peptide, there was no evidence of more than one binding site on either TAR RNA. Therefore, there is only one unique high-affinity specific binding site on the two TAR RNAs for L22 interactions. When L22 binds, the fluorescence intensities of HIV-1 P24, HIV-1 P25, and HIV-2 P25 all increase, similar to the direction of conformational changes induced by Tat at these positions upon complex formation.[6,7] However, the magnitude of the fluorescence change induced by L22 at HIV-1 P24 is greater than the magnitude of that induced by Tat, while the fluorescence changes at the other positions are comparable between Tat and L22. These changes observed from steady state fluorescence titration experiments again reflected only the population-averaged structural information but hinted at different responses that can be analyzed by ultrafast time-resolved dynamics probing to yield much more insightful population-resolved information to reveal the detailed mechanism of molecular recognition (see below).

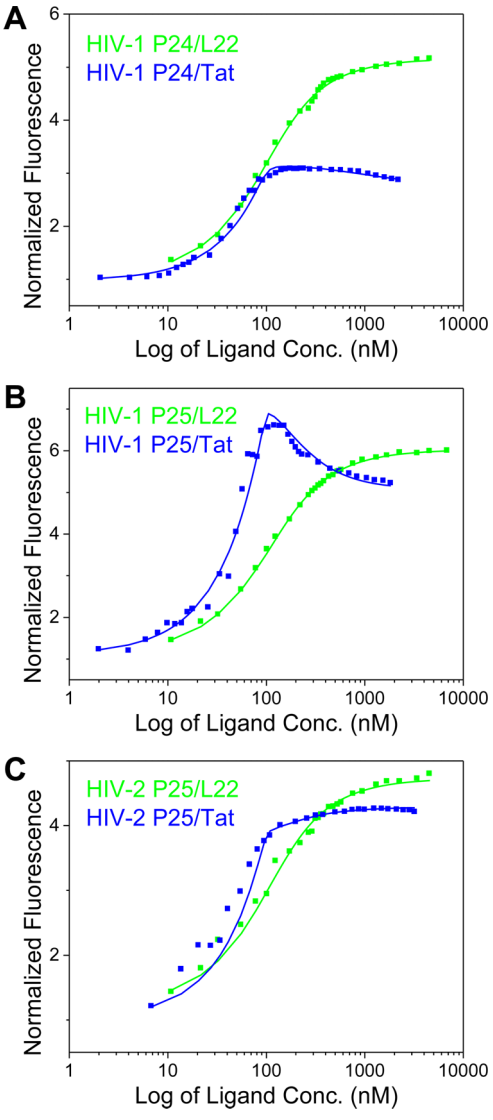

Figure 2. Steady state fluorescence titrations of Tat and L22 peptides binding to TAR RNAs (A) HIV-1 P24, (B) HIV-1 P25, and (C) HIV-2 P25.

Table 1. Dissociation Constants (K_d) of Tat and L22 Binding to HIV TAR RNAs

	Tat		L22
RNA construct	K_d1 (nM)	K_d2 (μM)	K_d (nM)
HIV-1 P24	60 ± 10	~1	44 ± 8
HIV-1 P25	6 ± 2	~0.1	63 ± 8
HIV-2 P25	~1	0.2 ± 0.05	63 ± 17

Conformational Heterogeneity of Bulge Residues of HIV TAR RNAs in the Free State. Structural studies have shown that looping out of the bulge bases is necessary for the formation of both HIV-1 and HIV-2 TAR−Tat complexes.[41−44] We have previously demonstrated that the ultrafast dynamics decays for the bulge bases in HIV-1 and HIV-2 TAR RNAs are heterogeneous in the free state, indicating the complexity of the conformational landscape for molecular recognition.[6,7] The multiphasic nature of these decay profiles for RNAs in the free state (Figure 3 and Table 2) indicated that these RNAs sample various heterogeneous conformations that are specific to virus strains and the base positions within the functionally important bulge.

In general, base 24 or 25 experiences differential base stacking interactions, or a lack of them, with surrounding bases within the bulge or with the closing base pairs, as well as dynamic motions of these bases in different unique conformational substates. These different types of base−base interactions and base motions were characterized by unique decay lifetimes of fluorophore 2AP in different local electronic environments that were captured by ultrafast dynamics (Table 2). The conformational equilibrium as the result of the conformational dynamics, reflected by the amplitudes of these characteristic lifetimes of the decay profiles, is established with low energy barriers (<1 kcal/mol) between the substates for interconversion that occur on time scales slower than the experimental technique of femtosecond dynamics.[6,7] Overall, there is a major subpopulation (50−70%) where the bulge bases stack continuously. This population of the highest occupancy represents the overall ground state for the ligand-free state, and this conformation is in equilibrium with other minor subpopulations where the bases dynamically flip out to some extent.

DOI: 10.1021/acs.biochem.5b00325
Biochemistry 2015, 54, 3687−3693

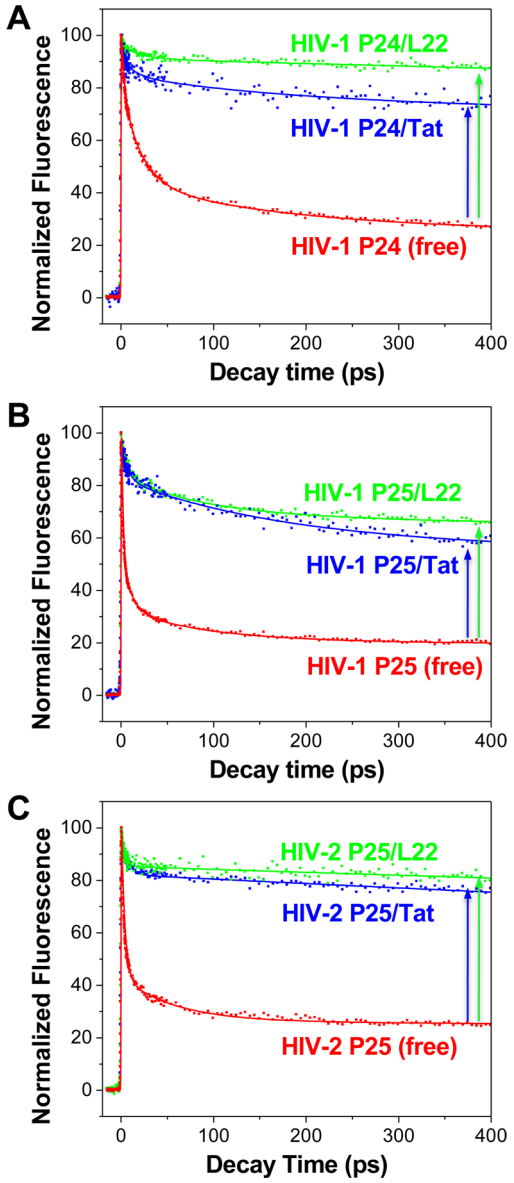

Figure 3. Ultrafast fluorescence time-resolved fluorescence decay profiles in the free state (red), Tat complex (blue), and L22 complex (green) for (A) HIV-1 P24, (B) HIV-1 P25, and (C) HIV-2 P25. Arrows indicate the direction and magnitude of changes in the dynamics decay profiles between Tat binding and L22 binding.

The transition between stacked and unstacked states plays a significant role in the conformational capture mechanism. Most importantly, the detection of bulge bases present in unstacked states by the femtosecond dynamics, represented by the lack of unique picoseccond ultrafast decay dynamics due to base stacking interactions,[6,7] offered strong and direct evidence that there are conformations within the ensemble for the free TAR RNA that resemble those of the RNA in the RNA–protein complexes. These results complemented those conducted by powerful NMR approaches[2,3,35−38] that revealed the plasticity of RNA on picosecond to nanosecond and microsecond to millisecond time scales to sample preexisting multiple conformations, including those similar to the ligand-bound states, underlying the notion that conformational capture[33,34] is the main mechanism of recognition in these RNA systems. Subsequently, we were interested in determining if there are any distinct dynamic signatures between Tat and L22 binding to TAR RNAs.

Table 2. Ultrafast Time-Resolved Dynamics Decay Parameters

RNA construct	free RNAs	TAR–Tat complexes	TAR–L22 complexes
HIV-1 P24	τ_1 = 3.3 ps, A_1 = 23%	τ_1 = 4.3 ps, A_1 = 5%	
	τ_2 = 21 ps, A_2 = 35%	τ_2 = 14 ps, A_2 = 6%	τ_1 = 20 ps, A_1 = 5%
	τ_3 = 170 ps, A_3 = 17%	τ_3 = 172 ps, A_3 = 10%	τ_2 = 0.96 ns, A_2 = 95%
	τ_4 = 11.3 ns, A_4 = 25%	τ_4 = 11.3 ns, A_4 = 79%	
HIV-1 P25	τ_1 = 1.9 ps, A_1 = 53%	τ_1 = 7.4 ps, A_1 = 13%	τ_1 = 6.6 ps, A_1 = 15%
	τ_2 = 9.6 ps, A_2 = 19%	τ_2 = 175 ps, A_2 = 26%	τ_2 = 88 ps, A_2 = 16%
	τ_3 = 92 ps, A_3 = 11%	τ_3 = 11.3 ns, A_3 = 61%	τ_3 = 11.3 ns, A_3 = 69%
	τ_4 = 11.3 ns, A_4 = 17%		
HIV-2 P25	τ_1 = 3.7 ps, A_1 = 61%	τ_1 = 7.0 ps, A_1 = 15%	τ_1 = 4 ps, A_1 = 16%
	τ_2 = 58 ps, A_2 = 15%	τ_2 = 4.7 ns, A_2 = 85%	τ_2 = 0.75 ns, A_2 = 84%
	τ_3 = 11.3 ns, A_3 = 24%		

Comparison of the Induced Conformational Transition in TAR RNAs between Tat and L22. The most powerful utility of using ultrafast dynamics to probe RNA conformational dynamics and the transition mechanism is the ability to provide a quantitative ensemble view of the resolved substates and the changes in the distribution of substates upon ligand binding,[23] as we have demonstrated in a number of RNA–ligand complex systems.[6,7,25,26,31,32] As we have shown previously, binding of Tat significantly changes the dynamics of the 2AP decay profiles for HIV-1 P24, HIV-1 P25, and HIV-2 P25 (Figure 3). The main changes are the significantly increased amplitudes of the slow nanosecond component, from 25 to 79%, 17 to 61%, and 24 to 85%, respectively, with concomitant decreased amplitudes of the ultrafast decay components, compared to those for the free state of the respective RNAs (Table 2). These observations on HIV TAR RNAs were interpreted as the bases sampling more unstacked states in the complex with Tat peptide, as the flipping out of these bases is necessary for specific structural features of complex formation.[41−44] Our current results form an interesting contrast to what was observed for 7SK RNA.[7] The 7SK RNA features a dinucleotide bulge region similar to that of HIV-2 TAR. Our femtosecond dynamics approach revealed that the conformation of the 7SK bulge region is also heterogeneous in the free state. Binding of Tat to 7SK, however, induced much smaller changes in the fluorescence decay dynamics profile, indicating the amplitudes of conformational changes are much smaller,[7] consistent with the notion that the bulge region is much more preorganized for Tat recognition.[45] For Tat complexes, although conformations with bulge bases flipping out are dominant in the complex, other conformations where the bases are still stacked with other bases can still be detected, underscoring the notion of conformational heterogeneity even in the more defined complex. Time-resolved anisotropy measurements also revealed base motions on the picosecond to nanosecond time scale that allow the

DOI: 10.1021/acs.biochem.5b00325
Biochemistry 2015, 54, 3687−3693

bases to sample various conformations within a shallow energy well.[6]

Similar to that of Tat, binding of L22 to the HIV TAR RNAs also induced large changes in the decay profiles (Figure 3). For HIV-1 P24, the profile for the L22 complex is mostly flat within the experimental time window, with a 0.96 ns component being the overwhelmingly dominant decay component (95%), and there is only a very small component on the ultrafast time scale (20 ps, 5%). The amplitude of the slow component is significantly larger than that of the Tat complex (79%). This suggests that L22 shifts the equilibrium of base 24 in HIV-1 TAR RNA almost completely toward the bulged out state compared to the extent induced by Tat. The NMR structure of the HIV-1 TAR–L22 complex[19] showed that base 24 is mostly buried in a hydrophobic pocket formed by the side chains of L22, and this sequestration of the base is responsible for the more complete decay, as well as the shortened lifetime of 2AP in a hydrophobic environment compared to exposure to an aqueous environment.[46]

In contrast to base 24 of HIV-1 TAR, L22 induces similar changes to the profiles of base P25 in both HIV-1 and HIV-2 TAR RNAs compared to linear Tat peptide. HIV-1 P25 and HIV-2 P25 have similar decay profiles in the free state. HIV-1 P25–L22 and HIV-2 P25–L22 complexes feature 69 and 84% slow nanosecond components, compared to 61 and 85% for Tat complexes, respectively. U25 was shown to protrude into solution similarly in both Tat and L22 complexes.[19] The extruded base can transiently interact with other bases in some minor subpopulation, causing the fluorescence to decay on ultrafast time scales.

It has been shown that the different bulge bases may serve somewhat different roles for the conformational transition; e.g., base 24 in HIV-1 TAR and base 25 in HIV-2 TAR serve mostly as a linker region,[6,7] where base 25 of HIV-1 TAR has a more critical structural role.[6,47−49] Taken together, it appears that both the natural Tat peptide and the designed cyclic mimic Tat of L22 interact with the two different types of bulge residues with different efficiencies of shifting the populations.

CONCLUSIONS

In this work, we demonstrate that a designed cyclic peptide mimic of HIV Tat peptide can specifically recognize HIV TAR RNAs with a single binding site, compared to two binding sites for Tat using our unique ultrafast dynamics approach. Our study provides more intricate details of the TAR RNA conformational transition patterns, capturing not only the major subpopulations but also minor subpopulations, painting the conformational transition with an ensemble view. Targeting RNAs as a new way of therapeutic intervention of viral diseases has been challenging,[18,50−52] but our study using peptidomimetics will narrow the gaps in this field by providing a unique strategy for identifying the properties of novel drug leads. Although both Tat and L22 bind the TAR RNAs as β-hairpin structures, cyclization in L22 affords a more efficient ligand from a population shifting perspective. Because such a population shift is necessary for specific ligand binding, lessons learned from this study can provide insights into how to better design novel drugs such as cyclic peptoids with potential TAR RNA binding affinity to differentiate similar structures on the basis of distinct dynamic behaviors. Our research will pave the way for the discovery of novel molecules for treatment of the HIV/AIDS pandemic.

AUTHOR INFORMATION

Corresponding Author

*Department of Medicinal Chemistry, College of Pharmacy, University of Florida, Gainesville, FL 32610. E-mail: xqi@cop.ufl.edu. Telephone: (352) 294-5581. Fax: (352) 392-9455.

Funding

This work was supported by a University of Florida Emerging Pathogens Institute Seed Grant to X.Q. and in part by National Institutes of Health/National Center for Advancing Translational Sciences Clinical and Translational Science Award UL1 TR00064 to the University of Florida.

Notes

The authors declare no competing financial interest.

ACKNOWLEDGMENTS

We thank Dr. Gabriele Varani for providing the initial sample of L22 peptide for testing.

ABBREVIATIONS

TAR, transactivation response; Tat, transactivator of transcription; PAGE, polyacrylamide gel electrophoresis; 2AP, 2-aminopurine; fwhm, full width at half-maximum; OPA, optical parametric amplifier.

REFERENCES

(1) Al-Hashimi, H. M. (2005) Dynamics-based amplification of RNA function and its characterization by using NMR spectroscopy. *ChemBioChem 6*, 1506−1519.

(2) Zhang, Q., Sun, X. Y., Watt, E. D., and Al-Hashimi, H. M. (2006) Resolving the motional modes that code for RNA adaptation. *Science 311*, 653−656.

(3) Zhang, Q., Stelzer, A. C., Fisher, C. K., and Al-Hashimi, H. M. (2007) Visualizing spatially correlated dynamics that directs RNA conformational transitions. *Nature 450*, 1263−1267.

(4) Edwards, T. E., Okonogi, T. M., Robinson, B. H., and Sigurdsson, S. T. (2001) Site-specific incorporation of nitroxide spin-labels into internal sites of the TAR RNA; structure-dependent dynamics of RNA by EPR spectroscopy. *J. Am. Chem. Soc. 123*, 1527−1528.

(5) Musiani, F., Rossetti, G., Capece, L., Gerger, T. M., Micheletti, C., Varani, G., and Carloni, P. (2014) Molecular Dynamics Simulations Identify Time Scale of Conformational Changes Responsible for Conformational Selection in Molecular Recognition of HIV-1 Transactivation Responsive RNA. *J. Am. Chem. Soc. 136*, 15631−15637.

(6) Lu, J., Kadakkuzha, B. M., Zhao, L., Fan, M., Qi, X., and Xia, T. (2011) Dynamic ensemble view of the conformational landscape of HIV-1 TAR RNA and allosteric recognition. *Biochemistry 50*, 5042−5057.

(7) Lu, J., Wong, V., Zhang, Y., Tran, T., Zhao, L., Xia, A., Xia, T., and Qi, X. (2014) Distinct conformational transition patterns of noncoding 7SK snRNA and HIV TAR RNAs upon Tat binding. *Biochemistry 53*, 675−681.

(8) Hamy, F., Felder, E. R., Heizmann, G., Lazdins, J., Aboul-ela, F., Varani, G., Karn, J., and Klimkait, T. (1997) An inhibitor of the Tat/TAR RNA interaction that effectively suppresses HIV-1 replication. *Proc. Natl. Acad. Sci. U.S.A. 94*, 3548−3553.

(9) Daelemans, D., Schols, D., Witvrouw, M., Pannecouque, C., Hatse, S., van Dooren, S., Hamy, F., Klimkait, T., de Clercq, E., and VanDamme, A. M. (2000) A second target for the peptoid Tat/transactivation response element inhibitor CGP64222: Inhibition of human immunodeficiency virus replication by blocking CXC-chemokine receptor 4-mediated virus entry. *Mol. Pharmacol. 57*, 116−124.

(10) Kesavan, V., Tamilarasu, N., Cao, H., and Rana, T. M. (2002) A new class of RNA-binding oligomers: Peptoid amide and ester analogues. *Bioconjugate Chem. 13*, 1171−1175.

DOI: 10.1021/acs.biochem.5b00325
Biochemistry 2015, 54, 3687−3693

(11) Huq, I., Wang, X., and Rana, T. M. (1997) Specific recognition of HIV-1 TAR RNA by a D-Tat peptide. *Nat. Struct. Biol. 4*, 881−882.
(12) Huq, I., Ping, Y. H., Tamilarasu, N., and Rana, T. M. (1999) Controlling human immunodeficiency virus type 1 gene expression by unnatural peptides. *Biochemistry 38*, 5172−5177.
(13) Gelman, M. A., Richter, S., Cao, H., Umezawa, N., Gellman, S. H., and Rana, T. M. (2003) Selective binding of TAR RNA by a Tat-derived β-peptide. *Org. Lett. 5*, 3563−3565.
(14) Runyon, S. T., and Puglisi, J. D. (2003) Design of a cyclic peptide that targets a viral RNA. *J. Am. Chem. Soc. 125*, 15704−15705.
(15) Athanassiou, Z., Dias, R. L., Moehle, K., Dobson, N., Varani, G., and Robinson, J. A. (2004) Structural mimicry of retroviral tat proteins by constrained β-hairpin peptidomimetics: Ligands with high affinity and selectivity for viral TAR RNA regulatory elements. *J. Am. Chem. Soc. 126*, 6906−6913.
(16) Leeper, T. C., Athanassiou, Z., Dias, R. L. A., Robinson, J. A., and Varani, G. (2005) TAR RNA recognition by a cyclic peptidomimetic of Tat protein. *Biochemistry 44*, 12362−12372.
(17) Athanassiou, Z., Patora, K., Dias, R. L., Moehle, K., Robinson, J. A., and Varani, G. (2007) Structure-guided peptidomimetic design leads to nanomolar β-hairpin inhibitors of the Tat-TAR interaction of bovine immunodeficiency virus. *Biochemistry 46*, 741−751.
(18) Bardaro, M. F., Shajani, Z., Patora-Komisarska, K., Robinson, J. A., and Varani, G. (2009) How binding of small molecule and peptide ligands to HIV-1 TAR alters the RNA motional landscape. *Nucleic Acids Res. 37*, 1529−1540.
(19) Davidson, A., Leeper, T. C., Athanassiou, Z., Patora-Komisarska, K., Karn, J., Robinson, J. A., and Varani, G. (2009) Simultaneous recognition of HIV-1 TAR RNA bulge and loop sequences by cyclic peptide mimics of Tat protein. *Proc. Natl. Acad. Sci. U.S.A. 106*, 11931−11936.
(20) Davidson, A., Patora-Komisarska, K., Robinson, J. A., and Varani, G. (2011) Essential structural requirements for specific recognition of HIV TAR RNA by peptide mimetics of Tat protein. *Nucleic Acids Res. 39*, 248−256.
(21) Lalonde, M. S., Lobritz, M. A., Ratcliff, A., Chamanian, M., Athanassiou, Z., Tyagi, M., Wong, J., Robinson, J. A., Karn, J., Varani, G., and Arts, E. J. (2011) Inhibition of Both HIV-1 Reverse Transcription and Gene Expression by a Cyclic Peptide that Binds the Tat-Transactivating Response Element (TAR) RNA. *PLoS Pathog. 7*, e1002038.
(22) Puglisi, J. D., Chen, L., Blanchard, S., and Frankel, A. D. (1995) Solution structure of a bovine immunodeficiency virus Tat-TAR peptide-RNA complex. *Science 270*, 1200−1203.
(23) Xia, T. (2008) Taking femtosecond snapshots of RNA conformational dynamics and complexity. *Curr. Opin. Chem. Biol. 12*, 604−611.
(24) Zhao, L., and Xia, T. (2009) Probing RNA Conformational Dynamics and Heterogeneity Using Femtosecond Time-resolved Fluorescence Spectroscopy. *Methods (Amsterdam, Neth.) 49*, 128−135.
(25) Xia, T., Becker, H. C., Wan, C., Frankel, A., Roberts, R. W., and Zewail, A. H. (2003) The RNA-protein complex: Direct probing of the interfacial recognition dynamics and its correlation with biological functions. *Proc. Natl. Acad. Sci. U.S.A. 100*, 8119−8123.
(26) Xia, T., Wan, C. Z., Roberts, R. W., and Zewail, A. H. (2005) RNA-protein recognition: Single-residue ultrafast dynamical control of structural specificity and function. *Proc. Natl. Acad. Sci. U.S.A. 102*, 13013−13018.
(27) Zhao, L., and Xia, T. (2007) Direct Revelation of Multiple Conformations in RNA by Femtosecond Dynamics. *J. Am. Chem. Soc. 129*, 4118−4119.
(28) Liu, J. D., Zhao, L., and Xia, T. (2008) The Dynamic Structural Basis of Differential Enhancement of Conformational Stability by 5′- and 3′-Dangling Ends in RNA. *Biochemistry 47*, 5962−5975.
(29) Kadakkuzha, B. M., Zhao, L., and Xia, T. (2009) Conformational Distribution and Ultrafast Base Dynamics of Leadzyme. *Biochemistry 48*, 3807−3809.
(30) Jain, N., Zhao, L., Liu, J. D., and Xia, T. B. (2010) Heterogeneity and Dynamics of the Ligand Recognition Mode in Purine-Sensing Riboswitches. *Biochemistry 49*, 3703−3714.
(31) Lee, S. W., Zhao, L., Pardi, A., and Xia, T. B. (2010) Ultrafast Dynamics Show That the Theophylline and 3-Methylxanthine Aptamers Employ a Conformational Capture Mechanism for Binding Their Ligands. *Biochemistry 49*, 2943−2951.
(32) Lu, J., Zhao, L., Xia, A., Xia, T., and Qi, X. (2013) Dissect Conformational Distribution and Drug-Induced Population Shift of Prokaryotic rRNA A-Site. *Biochemistry 52*, 1651−1653.
(33) Leulliot, N., and Varani, G. (2001) Current topics in RNA-protein recognition: Control of specificity and biological function through induced fit and conformational capture. *Biochemistry 40*, 7947−7956.
(34) Williamson, J. R. (2000) Induced fit in RNA-protein recognition. *Nat. Struct. Biol. 7*, 834−837.
(35) Al-Hashimi, H. M., and Walter, N. G. (2008) RNA dynamics: It is about time. *Curr. Opin. Struct. Biol. 18*, 321−329.
(36) Frank, A. T., Stelzer, A. C., Al-Hashimi, H. M., and Andricioaei, I. (2009) Constructing RNA dynamical ensembles by combining MD and motionally decoupled NMR RDCs: New insights into RNA dynamics and adaptive ligand recognition. *Nucleic Acids Res. 37*, 3670−3679.
(37) Al-Hashimi, H. M., Gosser, Y., Gorin, A., Hu, W. D., Majumdar, A., and Patel, D. J. (2002) Concerted motions in HIV-1 TAR RNA may allow access to bound state conformations: RNA dynamics from NMR residual dipolar couplings. *J. Mol. Biol. 315*, 95−102.
(38) Bailor, M. H., Sun, X., and Al-Hashimi, H. M. (2010) Topology links RNA secondary structure with global conformation, dynamics, and adaptation. *Science 327*, 202−206.
(39) Andrushchenko, V. V., Vogel, H. J., and Prenner, E. J. (2007) Optimization of the hydrochloric acid concentration used for trifluoroacetate removal from synthetic peptides. *J. Pept. Sci. 13*, 37−43.
(40) Kuzmic, P. (1996) Program DYNAFIT for the analysis of enzyme kinetic data: Application to HIV proteinase. *Anal. Biochem. 237*, 260−273.
(41) Puglisi, J. D., Tan, R., Calnan, B. J., Frankel, A. D., and Williamson, J. R. (1992) Conformation of the TAR RNA-arginine complex by NMR spectroscopy. *Science 257*, 76−80.
(42) Aboul-ela, F., Karn, J., and Varani, G. (1995) The Structure of the Human Immunodeficiency Virus Type-1 TAR RNA Reveals Principles of RNA Recognition by Tat Protein. *J. Mol. Biol. 253*, 313−332.
(43) Puglisi, J. D., Chen, L., Frankel, A. D., and Williamson, J. R. (1993) Role of RNA structure in arginine recognition of TAR RNA. *Proc. Natl. Acad. Sci. U.S.A. 90*, 3680−3684.
(44) Brodsky, A. S., and Williamson, J. R. (1997) Solution structure of the HIV-2 TAR-argininamide complex. *J. Mol. Biol. 267*, 624−639.
(45) Durney, M. A., and D'Souza, V. M. (2010) Preformed protein-binding motifs in 7SK snRNA: Structural and thermodynamic comparisons with retroviral TAR. *J. Mol. Biol. 404*, 555−567.
(46) Ward, D. C., Reich, E., and Stryer, L. (1969) Fluorescence studies of nucleotides and polynucleotides. I. Formycin, 2-aminopurine riboside, 2,6-diaminopurine riboside, and their derivatives. *J. Biol. Chem. 244*, 1228−1237.
(47) Weeks, K. M., Ampe, C., Schultz, S. C., Steitz, T. A., and Crothers, D. M. (1990) Fragments of the HIV-1 Tat Protein Specifically Bind TAR RNA. *Science 249*, 1281−1285.
(48) Weeks, K. M., and Crothers, D. M. (1992) RNA-Binding Assays for Tat-Derived Peptides: Implications for Specificity. *Biochemistry 31*, 10281−10287.
(49) Aboul-ela, F., Karn, J., and Varani, G. (1996) Structure of HIV-1 TAB RNA in the absence of ligands reveals a novel conformation of the trinucleotide bulge. *Nucleic Acids Res. 24*, 3974−3981.
(50) Stelzer, A. C., Frank, A. T., Kratz, J. D., Swanson, M. D., Gonzalez-Hernandez, M. J., Lee, J., Andricioaei, I., Markovitz, D. M., and Al-Hashimi, H. M. (2011) Discovery of selective bioactive small

DOI: 10.1021/acs.biochem.5b00325
Biochemistry 2015, 54, 3687−3693

molecules by targeting an RNA dynamic ensemble. *Nat. Chem. Biol. 7*, 553−559.
(51) Davidson, A., Begley, D. W., Lau, C., and Varani, G. (2011) A Small-Molecule Probe Induces a Conformation in HIV TAR RNA Capable of Binding Drug-Like Fragments. *J. Mol. Biol. 410*, 984−996.
(52) Tran, T., and Disney, M. D. (2010) Two-dimensional combinatorial screening of a bacterial rRNA A-site-like motif library: Defining privileged asymmetric internal loops that bind aminoglycosides. *Biochemistry 49*, 1833−1842.

DOI: 10.1021/acs.biochem.5b00325
Biochemistry 2015, 54, 3687−3693